JOURNAL OF THERMOPHYSICS AND HEAT TRANSFER
Vol. 19, No. 1, January–March 2005

Heat Transfer in Rotating Rectangular Channels with V-Shaped and Angled Ribs

Eungsuk Lee,* Lesley M. Wright,* and Je-Chin Han†
Texas A&M University, College Station, Texas 77843-3123

An experimental study was performed to measure the regionally averaged heat-transfer distributions in a rotating ribbed channel with an aspect ratio of 4:1. The Reynolds number, based on hydraulic diameter, varies from 5×10^3 to 40×10^3. The rotation number ranges from 0 to 0.3, and the inlet coolant-to-wall density ratio ($\Delta\rho/\rho$) is maintained around 0.122. Six different configurations of ribs, oriented at an angle of 45 deg to the direction of flow, are placed on both the leading and trailing surfaces: 1) parallel V-shaped ribs without gaps, 2) staggered V-shaped ribs without gaps, 3) parallel V-shaped ribs with gaps, 4) parallel angled ribs without gaps, 5) staggered angled ribs without gaps, and 6) parallel angled ribs with gaps. The rib-height-to-hydraulic-diameter ratio (e/D_h) is 0.078, and the rib-pitch-to-height ratio (P/e) is 10. The channel orientation with respect to the plane of rotation is 135 deg. The results show that the V-shaped rib configuration produces more heat-transfer enhancement than the angled rib configurations. It is also shown that there is only a negligible difference between the heat-transfer enhancement due to the staggered V-shaped ribs without gaps and the enhancement due to the parallel V-shaped ribs without gaps. The same is true for the staggered and parallel angled ribs without gaps. Also, the parallel V-shaped ribs without gaps produce more heat-transfer enhancement than the V-shaped ribs with gaps, whereas the parallel angled ribs with gaps produce more heat-transfer enhancement than the angled ribs without gaps. Finally, rotation further increases the heat transfer from all surfaces above that of the stationary channels.

Nomenclature

AR	=	channel aspect ratio, $W:H$
A	=	surface area of copper plate, m^2
D_h	=	hydraulic diameter, m
e	=	rib height, m
H	=	channel height, m
h	=	convective heat transfer coefficient, W/m^{2}K
k	=	thermal conductivity of coolant, W/m K
L	=	heated length of channel, m
Nu	=	regionally averaged Nusselt number, hD_h/k
Nu_0	=	Nusselt number for flow in fully developed turbulent nonrotating smooth tube
P	=	rib pitch, m
Pr	=	Prandtl number
Q_{net}	=	net heat transfer rate, W
q''_{net}	=	net heat flux at wall, W/m^2
R	=	mean rotating arm radius, cm
Re	=	Reynolds number, $\rho V D_h/\mu$
Ro	=	Rotation number, $\Omega D_h/V$
T_{bi}	=	coolant temperature at inlet, K
T_{bx}	=	local coolant bulk temperature, K
T_w	=	wall temperature, K
V	=	bulk velocity in streamwise direction, m/s
W	=	channel width, m
α	=	rib angle
β	=	angle of channel orientation
ρ	=	density of coolant, kg/m^3
$\Delta\rho/\rho$	=	inlet coolant-to-wall density ratio, $(\rho_{bi} - \rho_w)/\rho_{bi} = (T_w - T_{bi})/T_w$
Ω	=	rotational speed, rad/s

Introduction

TO achieve higher thermal efficiency and power output in advanced gas turbines, rotor inlet temperatures may need to exceed the melting point of the blade material. Therefore, it is necessary to remove the thermal energy for safe and long operation of the turbine. Internal cooling is one method for cooling the turbine blade. With internal cooling, pressurized cooling air is extracted from the compressor and injected into the turbine blade. The coolant circulates through cooling passages to remove heat from the blade.

Numerous techniques have been employed to enhance the heat transfer within the internal cooling passages. The channel walls are typically lined with turbulence promoters to increase the heat transfer from the channel walls to the coolant. The cooling passages may utilize rib turbulators (trip strips), pin-fins, or dimples to enhance the heat transfer. Rib-turbulated cooling is commonly used in modern engines, and because ribs are widely used for heat-transfer enhancement, many experimental investigations have been completed to examine the level of heat-transfer enhancement in ribbed channels. To begin to understand the complexities of internal cooling in turbine blades, many experiments have been performed that model the internal cooling passages as stationary channels. The interested reader is referred to *Gas Turbine Heat Transfer and Cooling Technology*[1] for a comprehensive review of internal cooling. The book includes numerous studies that have been conducted over the years on a wide range of rib configurations in cooling channels of various sizes using many experimental techniques. However, the flowfield through a rotating channel exhibits different characteristics than the flowfield through a stationary channel. This is due to the forces generated by rotation. These Coriolis and rotational buoyancy forces shift the peak velocity of the coolant toward the trailing surface of the blade in a passage with radial outflow. Therefore, the coolant is forced away from the leading surface (suction side) of the channel to the trailing surface (pressure side). Typically, under rotation, the trailing surface experiences heat-transfer enhancement, whereas the leading surface experiences a reduction in heat transfer.

The duct orientation and aspect ratio also have an effect on the coolant flow through the channel. As shown in Fig. 1, as one moves

Received 14 March 2004; revision received 22 June 2004; accepted for publication 22 June 2004.

*Graduate Research Assistant, Turbine Heat Transfer Laboratory, Department of Mechanical Engineering.

†M.C. Easterling Chair Professor, Turbine Heat Transfer Laboratory, Department of Mechanical Engineering; jchan@mengr.tamu.edu. Associate Fellow AIAA.

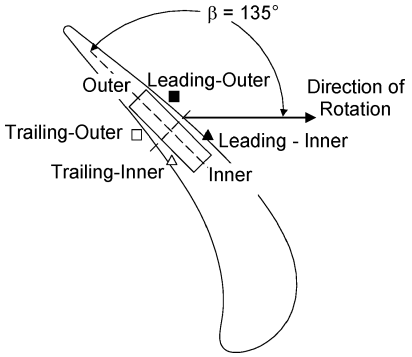

Fig. 1 Orientation and surface legend of a rectangular channel (AR = 4:1) in a gas-turbine blade.

from the midchord of the blade toward the trailing edge, the blade becomes thinner; therefore, cooling channels must become narrower (the aspect ratio increases). Moving toward the trailing edge of the blade also alters the orientation angle (β) of the cooling channel. From the midchord to the trailing edge, the orientation angle (measured from the direction of rotation to the midpoint of the channel) increases. For narrow ducts with large orientation angles, the coolant is forced away from the leading and inner surfaces toward the trailing and outer surfaces of the channel during rotation. Figure 1 also shows the orientation of a 4:1-aspect-ratio channel within the trailing edge of a turbine blade.

Early studies investigated cooling channels with orthogonal ribs.[2] It was then determined that placing the ribs at an angle to the mainstream flow would result in greater heat-transfer enhancement than for ribs positioned at 90 deg to the mainstream flow. Studies by Han and Park[3] and Park et al.[4] investigated the heat-transfer enhancement of angled ribs over orthogonal ribs. The results showed that the heat-transfer enhancement in angled-rib channels is significantly greater than the heat-transfer enhancement due to normal ribs.

The focus of rib turbulator investigations began to shift to "high-performance" ribs. Han et al.[5] studied a square channel with V, Λ, parallel (angled), and crossed ribs. They showed that the V-shaped ribs (45 and 60 deg) result in more heat-transfer enhancement than the parallel ribs (45 and 60 deg). Similarly, using the mass-transfer technique, Lau et al.[6] found that the V-shaped ribs create greater heat-transfer enhancement than full (angled) angled ribs.

Han and Zhang[7] then completed a study of a square channel with various angled and V-shaped rib configurations. They concluded that broken ribs create heat-transfer enhancement levels of 2.5–4, whereas the enhancement level created by the continuous ribs is only 2–3. Taslim et al.[8] also studied various configurations of angled and V-shaped ribs using a liquid-crystal technique. They also concluded that V-shaped ribs result in the greatest heat-transfer enhancement. Ekkad and Han[9] also used a liquid-crystal technique to obtain detailed heat-transfer distributions in a two-pass channel with parallel (angled), V-shaped, and broken V-shaped (discrete V-shaped) ribs. They concluded that the parallel, V-shaped, and broken V-shaped ribs produce similar heat-transfer enhancement, with the broken V-shaped ribs giving slightly higher enhancement.

Cho et al.[10] recently investigated angled and discrete-angled ribs using mass transfer. They concluded that the heat-transfer performance of the discrete ribs is similar to that of the angled ribs in a rectangular channel with an aspect ratio of 2.04:1. A very narrow channel ($AR = 8{:}1$) with V-shaped, Λ-shaped, and angled ribs was studied by Gao and Suden.[11] Using a liquid-crystal technique, they too confirmed that V-shaped ribs result in the highest heat-transfer enhancement. Rhee et al.[12] also investigated rectangular channels ($AR = 3{:}1$, 5:1, and 6.82:1). They studied the heat-transfer enhancement of V-shaped and discrete V-shaped ribs. Based on their configurations, they concluded that the thermal performance of the two configurations was comparable.

All of the above studies focus on the performance of various configurations of ribs in nonrotating channels. Many studies have been performed that investigate the effect of rotation on cooling channels. Johnson et al.[13] experimentally investigated heat transfer in multipass rotating channels with angled ribs. With multipass channels, the coolant flows radially outward in the first pass, turns 180 deg, and then flows radially inward in the second pass; additional passes with alternating radial outward and inward flow can be used as needed. Johnson et al.[14] performed additional tests with this four-pass test duct to determine the effect of channel orientation on the heat-transfer enhancement. From these studies it was concluded that the heat transfer from both the leading and trailing surfaces of the ribbed channel was different from that in a nonrotating channel.

Parsons et al.[15,16] also studied the influence of channel orientation and wall-heating condition on the regionally averaged heat-transfer coefficients in a rotating two-pass square channel with 60- and 90-deg ribbed walls. This study showed that the heat-transfer coefficients are greater in channels that are maintained at a constant wall temperature. They found this difference is greater for the channel oriented at 45 deg than for the channel oriented perpendicular to the direction of rotation.

Dutta and Han[17] conducted an experimental study of regionally averaged heat-transfer coefficients in rotating smooth and ribbed two-pass channels with three channel orientations. They found that the effect of rotation is reduced for nonorthogonal alignment of the heat-transfer surfaces with respect to the plane of rotation. They also concluded that the staggered half V-shaped ribs have better heat-transfer performance than the 90-deg ribs and the 60-deg angled ribs.

Park et al.[18,19] conducted naphthalene sublimation experiments to examine the effects of rotation on the local heat- and mass-transfer distribution in a two-pass ribbed square channel. They also found that the overall heat and mass transfer in a rotating channel with ribbed surfaces was not affected by the Coriolis force as much as that in a rotating channel with smooth surfaces.

Taslim et al.[20,21] investigated the heat-transfer distribution in rotating square rib-roughened channels using a liquid-crystal technique. They found that the effects of rotation were more apparent in rib-roughened channels with a larger channel aspect ratio and a lower rib blockage ratio.

Due to the curved shape of turbine blades, cooling channels near the trailing edge are rectangular and the orientation angle of the channel increases. The heat-transfer trends in a square channel cannot be applied simply to rectangular channels. The effect of the Coriolis and rotational-buoyancy forces is altered by the larger aspect ratios and orientation angles. Recently, more studies have focused on these rectangular channels.

Kiml et al.[22] examined the heat transfer and pressure drop in a ribbed rectangular channel ($AR = 2{:}1$) for four rib configurations (90-, 75-, 60-, and 45-deg angled ribs). They revealed that 60-deg ribs produce the highest heat-transfer enhancement due to the strong rotational momentum of the rib-induced secondary flow. Kiml et al.[23] also investigated heat-transfer enhancement mechanisms in rectangular channels with V- and Λ-shaped ribs using a flow-visualization technique to examine the secondary flow behavior created by the V-shaped ribs.

Azad et al.[24] conducted an experimental study to determine heat-transfer enhancement in a rotating two-pass ribbed rectangular channel with an aspect ratio of 2:1. They showed that the heat transfer decreases from the leading surface and increases from the trailing surface for the first passage. They also found that the 90-deg channel orientation produces a greater rotation effect than the 135-deg channel orientation.

Al-Hadhrami and Han[25] and Al-Hadhrami et al.[26] studied the effect of rotation on heat transfer in rotating two-pass square and rectangular channels ($AR = 2{:}1$) with rib turbulators for two channel orientations. They found that the parallel and V-shaped ribs produced better heat-transfer enhancement than the crossed and inverted V-shaped ribs. They also found that parallel angled ribs produced better heat-transfer enhancement than crossed angled ribs. Furthermore, the 90-deg channel orientation produces a greater rotation effect on the heat transfer than a 135-deg channel orientation.

Griffith et al.[27] investigated the effect of rotation on heat transfer in a rib-roughened rectangular channel ($AR = 4{:}1$). They found that

the narrow rectangular passage exhibits much higher heat-transfer enhancement for the ribbed surfaces than the ribbed surfaces in a smaller-aspect-ratio channel. They also found spanwise heat-transfer distributions exist across the leading and trailing surfaces, and the variation is accentuated by the use of angled ribs. Also, they showed the orientation of the channel significantly affects the heat-transfer distribution.

More recent studies have begun to focus on the leading edge of the blade; these channels near the leading edge of the blades are taller ($H > W$) than the wide channels ($W > H$) located near the trailing edge. Cho et al.[28] used mass transfer to study the effect of rotation in a rotating two-pass rectangular channel ($AR = 1{:}2$) with 70-deg angled ribs. Agarwal et al.[29] used mass transfer to study a two-pass 1:4 rotating channel. In channels both with smooth walls and with 90-deg angled ribs, they found that the heat/mass transfer in the 1:4 channel is less than that in a square channel.

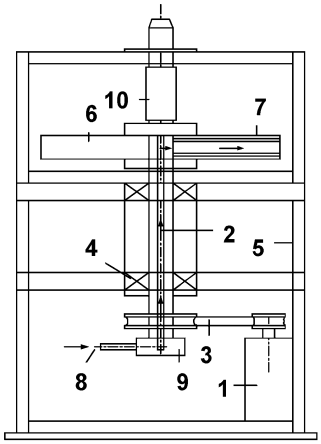

1- Variable Speed Electric Motor
2- Hollow Rotating Shaft
3- Belt-Driven Gear System
4- Bearing Support System
5- Steel Work Table
6 - Rotating Arm
7 - Test Section
8 - Compressor Air
9 - Rotary Seal
10 - Slip Ring Assembly

Fig. 2 Schematic of the rotating test rig.

Past studies showed that V-shaped ribs produce overall better heat-transfer enhancement than angled ribs. Although comparisons have been made to continuous and discrete ribs, no comparisons have been made between the performance of the ribs with gaps and without gaps. The gaps will allow any accumulated debris to be removed from the channel. Therefore, the channel should more effectively transfer heat from the blade wall to the coolant. Also, no comparison has been made between the performance of the parallel and staggered V-shaped or angled ribs. In this study, the regionally averaged heat-transfer distribution in a rotating rectangular channel with an aspect ratio of 4:1 is experimentally investigated. Six different rib configurations including parallel and staggered V-shaped ribs without gaps, parallel V-shaped ribs with gaps, parallel and staggered angled ribs without gaps, and parallel angled ribs with gaps are considered, and the performance of each rib configuration is compared with that of the others.

Experimental Setup

Figure 2 shows the experimental test rig. An electric motor with an adjustable frequency controller is connected to a hollow rotating shaft through a belt-driven gear system. The test section is inserted into one end of the rotating arm, and the other side of the arm serves to balance the rotating arm. A digital photo tachometer is used to measure the rotational velocity of the rotating arm. Compressed air (coolant) from a steady-flow compressor flows through an American Society of Mechanical Engineers orifice-flow meter, through the hollow rotating shaft, to the rotating arm, which is perpendicular

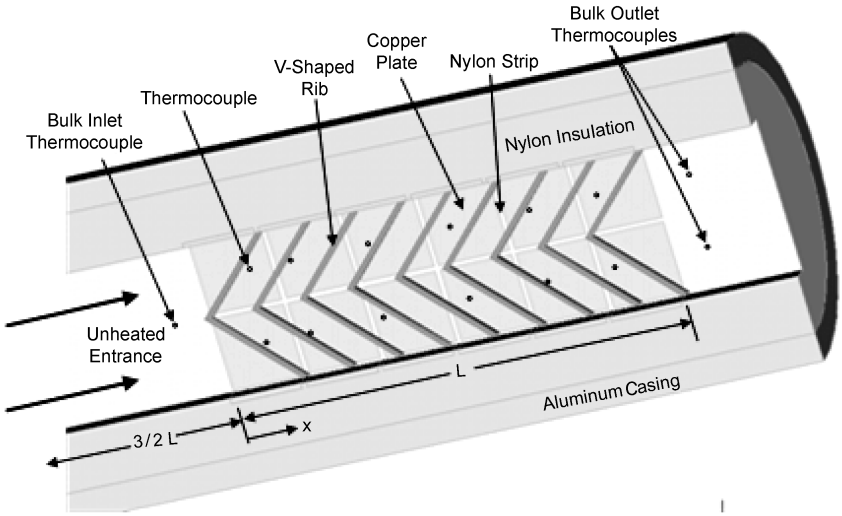

a) Top view of test section

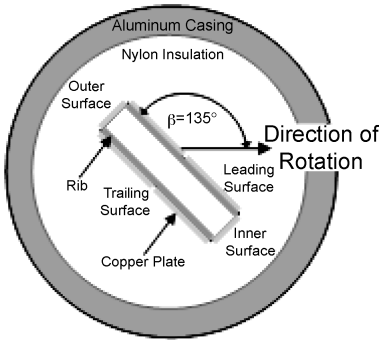

b) End view of test section

Fig. 3 Schematic of test section.

to the rotating shaft, through the test section, and is expelled to the atmosphere. Cooling air flows radially outward from the plane of rotation. The mean rotating-arm-radius-to-hydraulic-diameter ratio ($\bar{R}/D_h$) is 33.

Figure 3 shows the top view of the test section. The test section is a 0.5-in. (1.27-cm) by 2-in. (5.08-cm) one-pass rectangular channel with an aspect ratio of 4:1, and the channel orientation with respect to the direction of rotation is fixed at 135 deg. The test section consists of the leading, trailing, inner, and outer surfaces. Two rows of copper plates are placed on the leading and trailing surfaces to provide a grid for analysis of the spanwise variation in the regionally averaged heat-transfer coefficient. The channel-length-to-hydraulic-diameter ratio (L/D_h) is 7.5 with a ratio of 1:25 for each of the six cross-sections. There is a 0.0625-in. (0.159-cm) thin strip of nylon that acts as insulation between each two plates to prevent heat conduction between the plates. The copper plates are mounted in a nylon substrate, which composes the bulk of the test section. Prefabricated flexible heaters are installed beneath the leading and trailing surfaces, two for each surface. The outer and inner walls remain unheated. A blind hole is drilled on the backside of each plate, and a thermocouple is installed with thermal conducting glue in the hole.

A total of six ribbed channel geometries were considered in this study. The six configurations can be seen in Fig. 4. Three configurations of V-shaped ribs and three configurations of angled ribs were studied. The V-shaped rib configurations consist of parallel (in-line) ribs without gaps (continuous ribs), staggered (offset) ribs without gaps, and parallel ribs with gaps (partial V formation). These V-shaped rib configurations are shown in Figs. 4a–4c. Figures 4d–4f show similar arrangements of angled ribs. The angled-rib geometries also consist of parallel ribs without gaps, staggered ribs without gaps, and parallel ribs with gaps. For the ribbed channels with gaps, the length of the ribs is 80% of the length of the ribs without gaps. In other words, 10% was removed from each end of the ribs. The ribs are glued with a thin layer of thermal conducting glue to the leading and trailing surfaces of the channel. Therefore, there is only a negligible effect of thermal resistance between the ribs and the copper plates. The rib-height-to-hydraulic-diameter ratio (e/D_h) is 0.078 and the pitch-to-rib-height ratio (P/e) is 10. The experiments are conducted for Reynolds numbers of 5×10^3, 10×10^3, 20×10^3, and 40×10^3. The rotation speed is fixed at 550 rpm, so the rotation number (Ro) ranges from 0.04 to 0.3. The inlet coolant-to-wall density ratio ($\Delta\rho/\rho$) is maintained around 0.122.

Data Reduction

The objective of this investigation is to study the regionally averaged heat-transfer coefficient at various locations within the rotating rectangular channel. The heat-transfer coefficient is determined from the net heat-transfer rate per unit surface area, the regionally averaged temperature of the plate, and the local bulk mean air temperature. Therefore, the regionally averaged heat-transfer coefficient is calculated as

$$h = \frac{Q_{\text{net}}/A}{(T_w - T_{bx})} \tag{1}$$

The net heat flux (Q_{net}) is the electrical power supplied to the heaters minus the heat loss from the test section. The electrical power supplied to each heater is calculated from the measured voltage and heater resistance for each heater in the test section. The heat losses are determined under a no-flow condition by inserting insulation into the test section. By measuring the power supplied to the heaters and the temperature of each plate, the amount of heat being lost into the environment is determined from the conservation-of-energy principle. The ratio of the heat loss to the total heat input varies from 25% at a Reynolds number of 5×10^3 to 10% at a Reynolds number of 40×10^3. The surface area used in this study is the projected surface of the copper plate, neglecting the increase of the area by adding ribs. The regionally averaged wall temperature (T_w) is measured by the thermocouple installed in each plate. The local bulk mean air temperature (T_{bx}) is determined by a linear interpolation between the bulk air inlet and the average of the two outlet temperatures. The linear interpolation value of the local bulk air temperature can be checked by the energy-balance equation. Both methods compare well for the presented study. However, the linear interpolation method is used to calculate the local bulk air temperature. The energy-balance equation is

$$T_{bx} = T_{bi} + \sum_i (Q - Q_{\text{loss}})/mc_p, \qquad x = 1, 2, \ldots, 6 \tag{2}$$

The Dittus-Boelter/McAdams correlation is used to calculate the Nusselt number for fully developed flow through a smooth stationary circular tube and this correlation provides a common reference. The regionally averaged Nusselt number normalized byDittus-Boelter/McAdams is

$$Nu/Nu_0 = (hD_h/k)(1/0.023Re^{0.8}Pr^{0.4}) \tag{3}$$

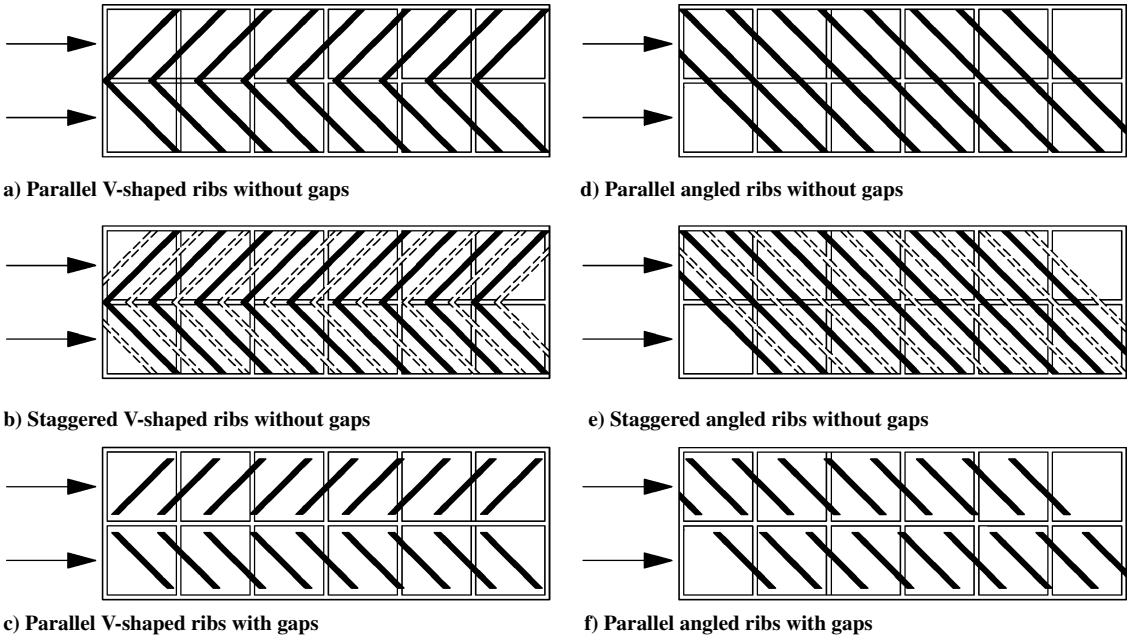

a) Parallel V-shaped ribs without gaps

d) Parallel angled ribs without gaps

b) Staggered V-shaped ribs without gaps

e) Staggered angled ribs without gaps

c) Parallel V-shaped ribs with gaps

f) Parallel angled ribs with gaps

Fig. 4 Top view of the six rib configurations.

All air properties are taken based on the mean bulk air temperature with a Prandtl number (Pr) for air of 0.71.

The experimental uncertainty for the presented results was calculated using the method developed and published by Kline and McClintock.[30] The estimated uncertainty in the temperature measurements is 0.5°C for all cases. At a Reynolds number of 5×10^3, the overall uncertainty in the Nusselt number ratio is approximately 23% of the presented values. At this lowest Reynolds number, a greater percentage of the heat input is lost. Due to the estimation of these heat losses, the experimental uncertainty increases. However, at the higher Reynolds numbers, the percentage uncertainty of the individual measurements decreases and the percentage of heat loss decreases. Therefore, the overall uncertainty in the Nusselt number ratio decreases to approximately 7% of the value calculated at the highest Reynolds number of 40×10^3.

Results and Discussion

Figure 1 shows the legend for the surfaces in a rectangular channel. The inner surface is closer to the midchord of the blade, and the outer surface is closer to the trailing edge of the blade. The leading surface is divided into the leading-inner and leading-outer surfaces, and the same is done for the trailing surface. With the narrow rectangular channel, the heat transfer from the inner and outer surfaces is much less than that from the leading and trailing surfaces, so the inner and outer surfaces were left unheated, but insulated.

Secondary-Flow Behavior

Figure 5 shows a conceptual view of the secondary-flow patterns induced by ribs, rotation, and channel orientation. For radially outward flow, the Coriolis forces induced by rotation produce a secondary flow that shifts the colder core flow toward the trailingmost corner of the channel, and it returns back to the leadingmost corner along either the trailing or the leading surface, creating two counter-rotating vortices. Therefore, the coolant near the trailingmost corner gradually becomes warmer as it moves toward the leadingmost corner. Consequently, the trailing-outer surface experiences the greatest heat-transfer enhancement.

Figure 5a shows the secondary flow induced by 45-deg V-shaped ribs and rotation. As the flow approaches the V-shaped ribs, it separates into two streams and each moves toward the inner or outer surfaces parallel to the ribs and returns to the centerline of the channel, creating two counter-rotating vortices. Thus the V-shaped ribs create four counter-rotating vortices in the cross section of the channel. Due to the symmetry of the ribs, it is expected that each surface will undergo the same amount of heat-transfer enhancement. Similar secondary flows induced by rotation, angled ribs, and V-shaped ribs in rectangular channels have been predicted from CFD predictions by Al-Qahtani et al.[31] and Su et al.[32]

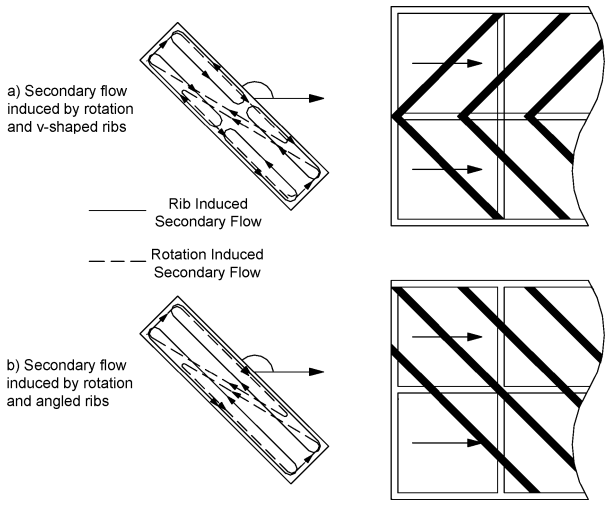

Fig. 5 Conceptual view of the secondary flows induced by rotation and ribs.

Figure 5b shows that the secondary flow induced by the 45-deg angled ribs moves parallel to the ribs from the outer surface to the inner surface and returns back to the outer surface. Thus, the angled ribs create two counter-rotating vortices rotating parallel to the angled ribs in the cross section of the channel. This secondary flow has the greatest velocity at the beginning of the rib and slows down as it travels along the rib surface. The faster secondary flow near the outer surfaces creates more turbulent mixing, so the heat from the outer surfaces is dissipated more effectively to the main bulk flow. Therefore, heat-transfer enhancement is expected to be greater for the leading- and trailing-outer surfaces than the leading- and trailing-inner surfaces due to the presence of the angled rib. The vortices induced by V-shaped ribs and the vortices induced by rotation rotate in the same direction. Thus, this produces constructive combinations of heat-transfer enhancement at the leading- and trailing-inner surfaces, whereas the vortices rotate in opposite directions and produce destructive combinations of heat-transfer enhancement at the leading- and trailing-outer surfaces. Angled-rib- and rotation-induced vortices rotate the same direction and produce constructive combinations of heat-transfer enhancement for all surfaces.

Regionally Averaged Heat-Transfer Results

Figures 6 and 7 contain the Nusselt number ratios for stationary and rotating ribbed channels, respectively. Each figure is subdivided into the six rib configurations 1) parallel V-shaped ribs, 2) staggered V-shaped ribs, 3) parallel V-shaped ribs with gaps, 4) parallel angled ribs, 5) staggered angled ribs, and 6) parallel angled ribs with gaps. Four Reynolds numbers were tested for both stationary and rotating cases. However, only one Reynolds number is represented in Figs. 6 and 7, $Re = 10 \times 10^3$; for the rotating cases, this corresponds to a rotation number of 0.150.

In the ribbed channel, the ribs act as turbulators and trip the boundary layer of the flow. This separation of the boundary layer results in a gradual development of the thermal boundary layer. The flow

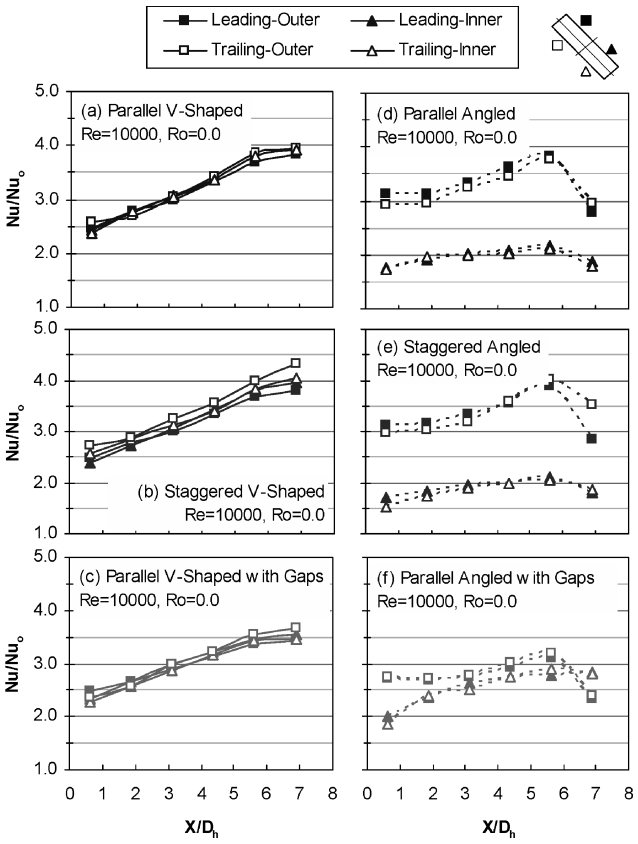

Fig. 6 Regionally averaged Nusselt number ratios in stationary channels.

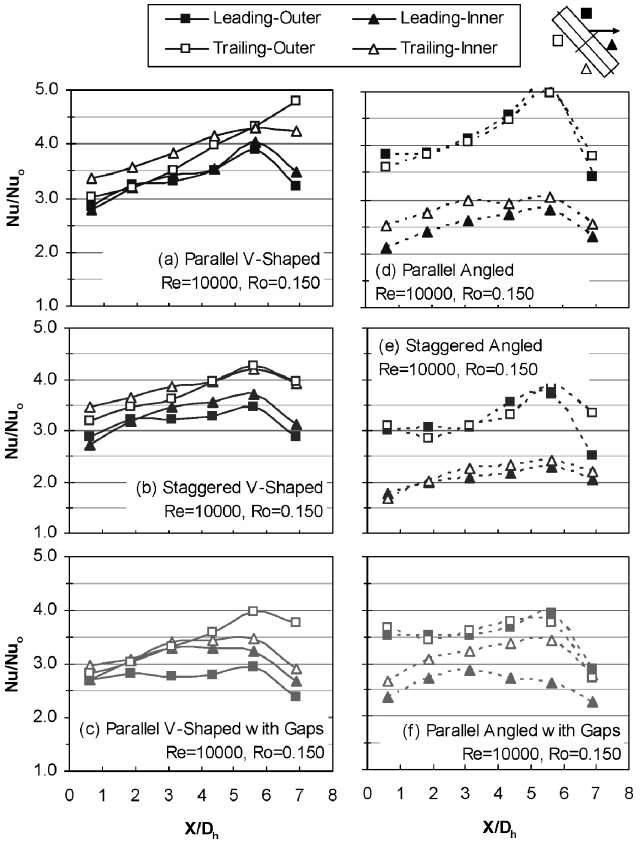

Fig. 7 Regionally averaged Nusselt number ratios in rotating channels.

becomes fully developed in the latter half of the channel. Figure 6 shows that the heat transfer gradually increases through the stationary channel as the rib-induced vortices become stronger until the flow becomes fully developed. Figure 6a shows the Nusselt number ratio for the stationary parallel V-shaped ribbed channel without gaps. Because of the symmetry of the channel all surfaces experience the same heat-transfer enhancement, and the results show that the variation of heat transfer between surfaces is less than 5%.

For the staggered-rib configuration, the blockage ratio is reduced, so the flow passes through the channel more readily. Therefore, it is expected that the staggered ribs will yield more heat-transfer enhancement and a smaller pressure drop than the parallel ribs. The trailing surfaces experience slightly higher heat-transfer enhancement than the leading surfaces for the stationary staggered V-shaped rib channel without gaps, as shown in Fig. 6b. This is due to the fact that the flow meets the first set of the ribs on the trailing surface before it meets the first set of the ribs on the leading surface, and the boundary-layer separation occurs earlier than on the leading surface. It can be also seen that there is a negligible difference in heat transfer between parallel- and staggered-rib configurations. The heat-transfer trends in the streamwise direction for the staggered V-shaped ribbed channel are similar to those for the parallel V-shaped ribbed channel (Fig. 6a).

The Nusselt number ratios for the parallel V-shaped ribbed channel with gaps are shown in Fig. 6c. It can be seen that V-shaped ribs with gaps produce approximately 10% less heat-transfer enhancement than parallel V-shaped ribs without gaps. The shorter ribs produce smaller rotating vortices than the rotating vortices created in the V-shaped ribbed channel without gaps. The smaller vortices produce weaker secondary flow, and thus reduce the overall heat-transfer enhancement, than the parallel V-shaped ribs without gaps.

Figure 6d shows the Nusselt number ratio for the stationary parallel angled ribbed channel without gaps. It is observed that the leading- and trailing-outer surfaces experience much more heat-transfer enhancement than the leading- and trailing-inner surfaces. This is due to the rib-induced secondary flow, as explained earlier. As with the V-shaped ribs, the Nusselt number ratio gradually increases as the counter-rotating vortices gain strength. The absence of the angled rib near the outlet for the leading- and trailing-outer surfaces leads to less turbulent mixing of the flow and a decrease in the Nusselt number.

Although a significant difference exists between the leading- and trailing-outer surfaces and the leading- and trailing-inner surfaces, the heat-transfer ratios for all of these surfaces are increasing at approximately the same rate as the rib-induced vortices gain strength. Although it is not shown, as the Reynolds number increases, the difference between the leading- and trailing-inner surfaces and the leading- and trailing-outer surfaces decreases. At increased Reynolds number, the flow is naturally turbulent, so the rib turbulators have less of an effect on the flow. Although there is separation of the leading- and trailing-inner and leading- and trailing-outer surfaces at high Reynolds numbers, the separation is much greater at the lower Reynolds numbers.

The heat-transfer trends in the streamwise direction for the staggered angled ribbed channel are the same as those for the parallel angled ribbed channel, as shown in Fig. 6e. As with the parallel and staggered V-shaped ribs, the difference between the heat-transfer enhancements due to the parallel and staggered angled ribs is negligible.

Figure 6f shows that the spanwise variation in heat transfer is reduced for the angled ribbed channel with gaps. The leading- and trailing-outer surfaces for the angled ribs with gaps experience less heat-transfer enhancement than for the angled ribs without gaps, and the leading- and trailing-inner surfaces experience much more heat-transfer enhancement than the angled ribbed channel without gaps. The secondary flow induced by the angled ribs with gaps is significantly different than the secondary flow induced by the angled ribs without gaps. In the angled ribbed channel without gaps, the ribs create two counter-rotating vortices that span the cross section of the channel. However, in the angled ribbed channel with gaps, a total of four vortices are created by the ribs. One set of the vortices is created along the leading- and trailing-outer surfaces. These vortices on the outer surfaces are created in the same manner as they are in the channel without gaps, but the length of the vortices is only as long as the rib itself. They do not extend the width of the channel. Due to the small vortices on the outer surfaces, these surfaces do not experience as much heat-transfer enhancement as the outer surfaces in the angled ribbed channel without gaps. A second set of vortices is created on the leading- and trailing-inner surfaces. These vortices force the coolant from the center of the channel toward the inner surface. The formation of this set of vortices allows relatively cooler air to circulate on the inner surfaces of the channel. This mixing of the coolant results in more heat-transfer enhancement from the leading- and trailing-inner surfaces in the angled ribbed channel with gaps than the angled ribbed channel without gaps.

Figure 7 contains the Nusselt number ratios for rotating ribbed channels. Similarly to Fig. 6, the heat-transfer enhancement is shown in each channel for a Reynolds number of 10×10^3 ($Ro = 0.150$). Figure 7a shows the Nusselt number ratio for the rotating V-shaped ribbed channel without gaps. It can be seen that the trailing-inner surface undergoes slightly higher heat-transfer enhancement than the trailing-outer surface. This is due to the fact that the rib- and rotation-induced secondary flows move in opposite directions, and the combined effects of these secondary flows are weakened. However, along the leading- and trailing-inner surfaces, both the rib- and rotation-induced secondary flows move in the same direction, and the combined effect of these secondary flows is strengthened. Although plots are not shown, similar trends exist for the other rotation numbers, and as the rotation number decreases (Reynolds number increases), the spanwise variation of the surfaces diminishes.

Figure 7b shows that the heat-transfer trends in the streamwise direction for the staggered V-shaped ribbed channel without gaps are the same as those for the parallel V-shaped ribbed channel without gaps (Fig. 7a). As with the stationary case (Fig. 6b), V-shaped ribs with gaps produce less heat-transfer enhancement than the V-shaped ribs without gaps, as shown in Fig. 7c.

The Nusselt number ratio for the rotating parallel-angled ribbed channel without gaps is shown in Fig. 7d. It can be seen that all surfaces undergo heat-transfer enhancement as compared to the stationary channel. This is due to the fact that the rib- and rotation-induced secondary flows move in the same direction and the combined effect of those secondary flows is strengthened. Because the coolant near the outer surface is colder than that near the inner surface, due to rotation, even more spanwise variation in heat transfer is observed. Also, the leading- and trailing-outer surfaces experience nearly the same heat-transfer enhancement, and the trailing-inner surface experiences higher heat-transfer enhancement than the leading-inner surface where the rotation-induced Coriolis forces are minimal. The heat-transfer trends in the streamwise direction for the rotating staggered-angled ribbed channel without gaps are the same as those for the rotating parallel-angled ribbed channel without gaps. This is seen in a comparison of Figs. 7d and 7e.

Figure 7f shows the Nusselt number ratio for the rotating parallel-angled ribbed channel with gaps. As with the stationary case (Fig. 6f), the spanwise variation in heat transfer is reduced. The Nusselt number ratios decrease for the leading- and trailing-outer surfaces, whereas they increase for the leading- and trailing-inner surfaces, as compared to the angled ribbed channel without gaps. Also, the difference in heat transfer between the leading-inner and the trailing-inner surface increases as the rotation number increases (this is clearly shown in later figures). From Fig. 7, it is observed that the heat-transfer enhancement by rotation is less than that by the ribs from the stationary smooth channel, and also, rotation does not alter the heat-transfer trends in the streamwise direction. Therefore, it can be concluded that the rotation-induced secondary flow is dominated by the rib-induced secondary flow.

Streamwise and Channel-Averaged Results

Figure 8 shows the channel-averaged Nusselt number ratio for the stationary smooth and ribbed channels. The results show that the heat transfer from the channel decreases as the Reynolds number increases. Also, it is clear there is only a slight difference in heat transfer between the parallel and staggered rib configurations. It can be seen that the V-shaped rib configurations produce more overall heat-transfer enhancement than the angled rib configurations. This is because the two sets of counter-rotating vortices, created by V-shaped ribs, allow more mixing of the flow and produce a thinner boundary layer near the surface. Also, the angled ribs with gaps experience higher overall heat-transfer enhancement than the angled ribs without gaps, due to the vortices created by the second half of the ribs.

The channel-averaged Nusselt number ratio for the different-aspect-ratio channels is also seen in Fig. 8. The rib-height-to-hydraulic-diameter ratio (e/D_h) is 0.094 for the rectangular channels ($AR = 2{:}1$) with V-shaped[26] and angled ribs without gaps[24] and 0.0625 for the square channels with V-shaped[5] and angled ribs without gaps.[5] The rib-pitch-to-height ratio (P/e) is 10 for all channels. In general, the square channel provides a greater heat-transfer enhancement than the rectangular channels. However, the rectangular channels do not provide a consistent trend. This could be due to the different rib-height-to-hydraulic-diameter ratio (e/D_h). The combined effect of the channel-aspect ratio and rib-height-to-hydraulic-diameter ratio on the heat-transfer enhancement needs further investigation and comparison.

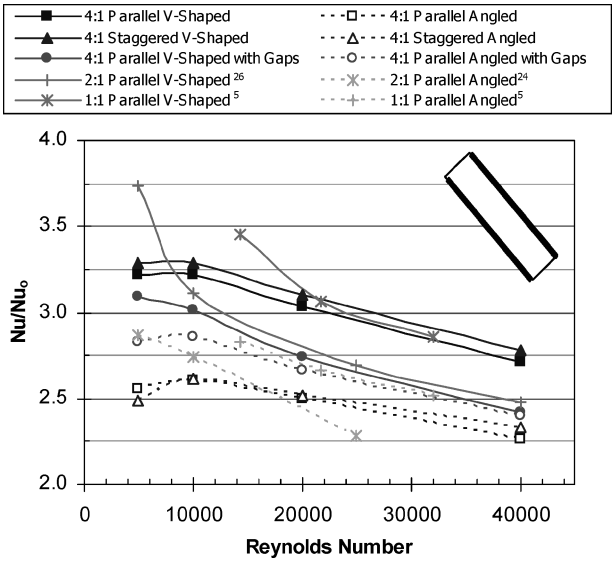

Fig. 8 Channel-averaged Nusselt number ratios in stationary channels.

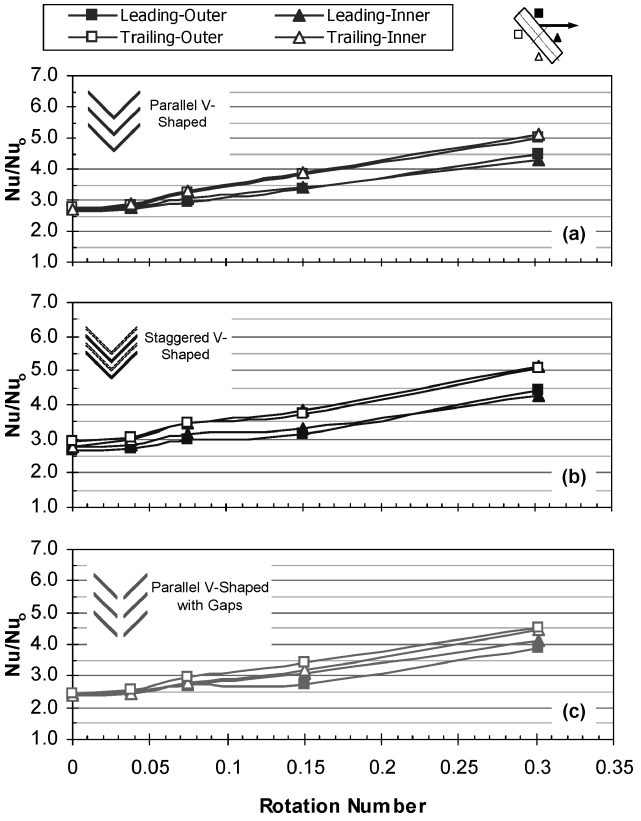

Fig. 9 Streamwise-averaged Nusselt number ratios in V-Shaped rib channels.

The streamwise-averaged Nusselt number ratios for the V-shaped ribbed channels can be seen in Fig. 9. For all cases, as the rotation number increases (Reynolds number decreases), the Nusselt number ratios increase. The trailing surfaces experience greater enhancement due to rotation than the leading surfaces. However, spanwise variation between the leading-outer and leading-inner surfaces is minimal; this is also true for the trailing-outer and trailing-inner surfaces.

Figure 10 shows the streamwise-averaged Nusselt number ratios for the angled ribbed channels. As the rotation number increases, the spanwise variation in heat transfer also increases due to the positive combined effect for the rib- and rotation-induced secondary flows, as explained previously. For the parallel-angled ribbed channel with gaps, the spanwise variation decreases, due to the vortex created by the second half of the ribs.

An interesting comparison of the ratios of the streamwise-averaged Nusselt numbers on the leading- and trailing-outer surfaces to those on the leading- and trailing-inner surfaces is made in Fig. 11. It can be seen that the angled rib configurations produce more overall heat-transfer enhancement than the V-shaped rib configurations for the leading- and trailing-outer surface due to the positive combined effects for the rib- and rotation-induced secondary flows, whereas the opposite is observed for the leading- and trailing-inner surfaces.

Figure 12 shows the channel-averaged Nusselt number ratio for the rotating smooth and ribbed channels as a function of the rotation number. The Nusselt-number ratios increase as the rotation number

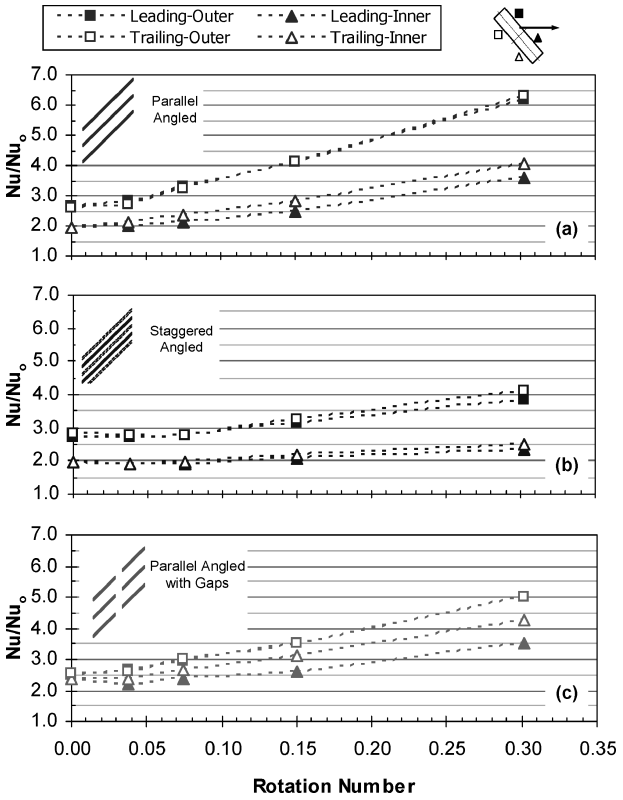

Fig. 10 Streamwise-averaged Nusselt number ratios in angled rib channels.

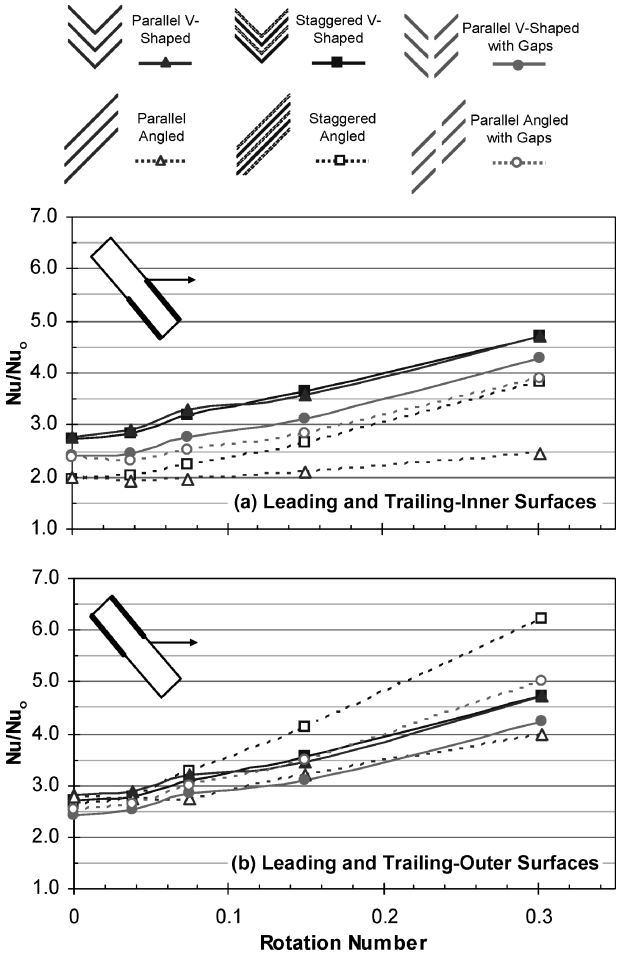

Fig. 11 Streamwise-averaged Nusselt number ratios for leading- and trailing-inner and -outer surfaces.

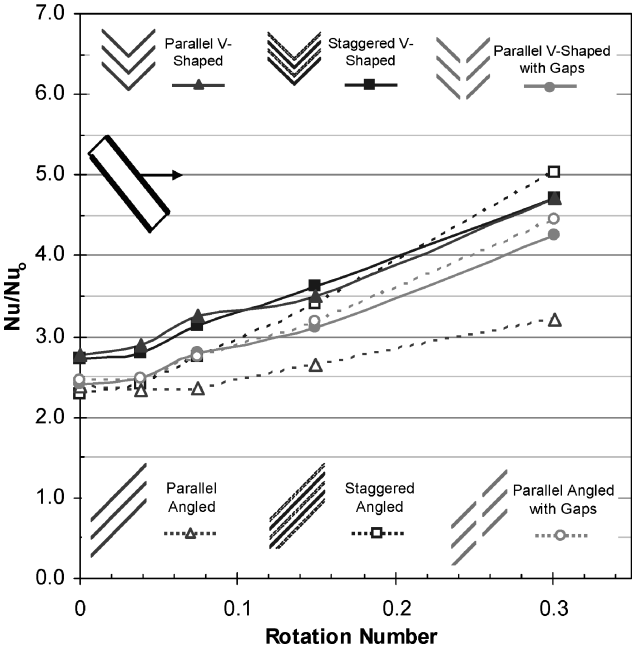

Fig. 12 Channel-averaged Nusselt number ratios in rotating channels.

increases for all channels. There is only a slight difference in heat transfer between parallel and staggered V-shaped ribbed channels without gaps. Also, the V-shaped ribbed channel without gaps produces more overall heat-transfer enhancement.

Conclusions

The cooling channels of modern gas-turbine blades vary in size and shape depending on their location in the blade. As the profile of the blade becomes narrower, the cooling channels must also become narrower, and the orientation with respect to the direction of rotation also changes. These relatively wide channels make it possible for a variety of rib configurations to be implemented to enhance the heat transfer from the blade wall. This study experimentally compared the heat-transfer enhancement of six different rib configurations: three V-shaped and three angled rib configurations. The study presents designers with new heat-transfer data applicable to the design of narrow cooling channels. From the results, the main conclusions are as follows:

1) For rotating narrow rectangular channels ($AR = 4{:}1$) with various V-shaped and angled ribs, heat-transfer enhancement on both the leading and trailing surfaces increases with rotation.

2) Significant spanwise variation of heat-transfer enhancement exists on both the leading and trailing surfaces in narrow rectangular channels ($AR = 4{:}1$) with various angled ribs. However, the spanwise variations decrease in rectangular channels with various V-shaped ribs.

3) V-shaped ribs produce more heat-transfer enhancement than angled ribs for both the stationary and rotating cases.

4) There is only a negligible difference in heat-transfer enhancement between the parallel and staggered rib configurations for both the stationary and rotating cases.

5) The V-shaped ribs with gaps produce less heat-transfer enhancement than the V-shaped ribs without gaps because of the shorter ribs, whereas the angled ribs with gaps produce greater heat-transfer enhancement than the angled ribs without gaps for both the stationary and rotating cases.

Acknowledgments

This publication was prepared with the support of the U.S. Department of Energy (DOE), Office of Fossil Energy, National Energy Technology Laboratory. However, any opinions, findings, conclusions, or recommendations expressed herein are those of the authors and do not necessarily reflect the views of the DOE.

References

[1]Han, J. C., Dutta, S., and Ekkad, S. V., *Gas Turbine Heat Transfer and Cooling Technology*, Taylor and Francis, New York, 2000, pp. 251–529.

[2]Han, J. C., "Heat Transfer and Friction Characteristics in Rectangular Channels with Rib Turbulators," *Journal of Heat Transfer*, Vol. 110, No. 2, 1988, pp. 321–328.

[3]Han, J. C., and Park, J. S., "Developing Heat Transfer in Rectangular Channels with Rib Turbulators," *International Journal of Heat and Mass Transfer*, Vol. 31, No. 1, 1988, pp. 183–195.

[4]Park, J. S., Han, J. C., Huang, Y., Ou, S., and Boyle, R. J., "Heat Transfer Performance Comparisons of Five Different Rectangular Channels with Parallel Angled Ribs," *International Journal of Heat and Mass Transfer*, Vol. 35, No. 11, 1992, pp. 2891–2903.

[5]Han, J. C., Zhang, Y. M., and Lee, C. P., "Augmented Heat Transfer in Square Channels with Parallel, Crossed, and V-Shaped Angled Ribs," *Journal of Heat Transfer*, Vol. 113, No. 3, 1991, pp. 590–596.

[6]Lau, S. C., Kukreja, R. T., and McMillin, R. D., "Effects of V-Shaped Rib Arrays on Turbulent Heat Transfer and Friction of Fully Developed Flow in a Square Channel," *International Journal of Heat and Mass Transfer*, Vol. 34, No. 7, 1991, pp. 1605–1616.

[7]Han, J. C., and Zhang, Y. M., "High Performance Heat Transfer Ducts with Parallel Broken and V-Shaped Broken Ribs," *International Journal of Heat and Mass Transfer*, Vol. 35, No. 2, 1992, pp. 513–523.

[8]Taslim, M. E., Li, T., and Kercher, D. M., "Experimental Heat Transfer and Friction in Channels Roughened with Angled, V-Shaped, and Discrete Ribs on Two Opposite Walls," *Journal of Turbomachinery*, Vol. 118, No. 1, 1996, pp. 20–28.

[9]Ekkad, S. V., and Han, J. C., "Detailed Heat Transfer Distribution in Two-Pass Square Channels with Rib Turbulators," *International Journal of Heat and Mass Transfer*, Vol. 40, No. 11, 1997, pp. 2525–2537.

[10]Cho, H. H., Wu, S. J., and Kwon, H. J., "Local Heat/Mass Transfer Measurements in a Rectangular Duct with Discrete Ribs," *Journal of Turbomachinery*, Vol. 122, No. 3, 2000, pp. 579–586.

[11]Gao, X., and Suden, B., "Heat Transfer and Pressure Drop Measurements in Rib-Roughened Rectangular Ducts," *Experimental Thermal and Fluid Science*, Vol. 24, No. 1, 2001, pp. 25–34.

[12]Rhee, D. H., Lee, D. H., Cho, H. H., and Moon, H. K., "Effects of Duct Aspect Ratios on Heat /Mass Transfer with Discrete V-Shaped Ribs," American Society of Mechanical Engineers, ASME Paper GT2003-38622, June 2003.

[13]Johnson, B. V., Wagner, J. H., Steuber, G. D., and Yeh, F. C., "Heat Transfer in Rotating Serpentine Passages with Trips Skewed to the Flow," *Journal of Turbomachinery*, Vol. 116, No. 1, 1994, pp. 113–123.

[14]Johnson, B. V., Wagner, J. H., Steuber, G. D., and Yeh, F. C., "Heat Transfer in Rotating Serpentine Passages with Selected Model Orientations for Smooth or Skewed Trip Walls," *Journal of Turbomachinery*, Vol. 116, No. 4, 1994, pp. 738–744.

[15]Parsons, J. A., Han, J. C., and Zhang, Y. M., "Wall Heating Effect on Local Heat Transfer in a Rotating Two-Pass Square Channel with 90° Rib Turbulators," *International Journal of Heat and Mass Transfer*, Vol. 37, No. 9, 1994, pp. 1141–1420.

[16]Parsons, J. A., Han, J. C., and Zhang, Y. M., "Effects of Model Orientation and Wall Heating Condition on Local Heat Transfer in a Rotating Two-Pass Square Channel with Rib Turbulators," *International Journal of Heat and Mass Transfer*, Vol. 38, No. 7, 1995, pp. 1151–1159.

[17]Dutta, S., and Han, J. C., "Local Heat Transfer in Rotating Smooth and Ribbed Two-Pass Square Channels with Three Channel Orientations," *Journal of Heat Transfer*, Vol. 118, No. 3, 1996, pp. 578–584.

[18]Park, C. W., Lau, S. C., Kukreja, R. T., "Heat/Mass Transfer in a Rotating Two-Pass Square Channel with Transverse Ribs," *Journal of Thermophysics and Heat Transfer*, Vol. 12, No. 1, 1998, pp. 80–86.

[19]Park, C. W., Yoon, C., Lau, S. C., "Heat (Mass) Transfer in a Diagonally Oriented Rotating Two-Pass Channels with Rib-Roughened Walls," *Journal of Heat Transfer*, Vol. 122, Feb. 2000, pp. 208–211.

[20]Taslim, M. E., Rahman, A., and Spring, S. D., "An Experimental Investigation of Heat Transfer Coefficients in a Span-Wise Rotating Channel with Two Opposite Rib-Roughened Walls," *Journal of Turbomachinery*, Vol. 113, No. 1, 1991, pp. 75–82.

[21]Taslim, M. E., Bondi, L. A., and Kercher, D. M., "An Experimental Investigation of Heat Transfer in an Orthogonally Rotating Channel Roughened with 45° Criss-Cross Ribs on Two Opposite Walls," *Journal of Turbomachinery*, Vol. 113, No. 3, 1991, pp. 346–353.

[22]Kiml, R., Mochizuki, S., and Murata, A., "Effects of Rib Arrangements on Heat Transfer and Flow Behavior in a Rectangular Rib-Roughened Passage: Application to Cooling of Gas Turbine Blade Trailing Edge," *Journal of Heat Transfer*, Vol. 123, No. 4, Aug. 2001, pp. 675–681.

[23]Kiml, R., Mochizuki, S., and Murata, A., "Heat Transfer Enhancement Mechanism in a Rectangular Passage with $\bar{V}$ and Λ Shaped Ribs," *Journal of Flow Visualization and Image Processing*, Vol. 8, No. 1, 2001, pp. 51–68.

[24]Azad, G. S., Uddin, M. J., Han, J. C., Moon, H. K., and Glezer, B., "Heat Transfer in a Two-Pass Rectangular Rotating Channel with 45-deg Angled Rib Turbulators," *Journal of Turbomachinery*, Vol. 124, No. 2, 2002, pp. 251–259.

[25]Al-Hadhrami, L., and Han, J. C., "Effect of Rotation in Two-Pass Square Channels with Five Different Orientations of 45° Angled Rib Turbulator," *International Journal of Heat and Mass Transfer*, Vol. 46, No. 4, 2003, pp. 653–669.

[26]Al-Hadhrami, L., Griffith, T. S., and Han, J. C., "Heat Transfer in Two-Pass Rotating Rectangular Channels ($AR = 2$) with Five Different Orientations of 45° V-Shaped Rib Turbulators," *Journal of Heat Transfer*, Vol. 125, No. 2, 2003, pp. 232–242.

[27]Griffith, T. S., Al-Hadhrami, L., and Han, J. C., "Heat Transfer in Rotating Rectangular Channels ($AR = 4$) with Angled Ribs," *Journal of Heat Transfer*, Vol. 124, No. 4, 2002, pp. 617–625.

[28]Cho, H. H., Kim, Y. Y., Kim, K. M., and Rhee, D. H., "Effects of Rib Arrangements and Rotation Speed on Heat Transfer in a Two-Pass Duct," American Society of Mechanical Engineers, ASME Paper GT2003-38609, June 2003.

[29]Agarwal, P., Acharya, S., and Nikitopoulos, D. E., "Heat/Mass Transfer in 1:4 Rectangular Passages with Rotation," American Society of Mechanical Engineers, ASME Paper GT2003-38615, June 2003.

[30]Kline, S. J., and McClintock, F. A., "Describing Uncertainties in Single-Sample Experiments," *Mechanical Engineering*, Vol. 75, Jan. 1953, pp. 3–8.

[31]Al-Qahtani, M., Jang, Y. J., Chen, H. C., and Han, J. C., "Prediction of Flow and Heat Transfer in Rotating Two-Pass Rectangular Channels with 45-Deg Rib Turbulators," *Journal of Turbomachinery*, Vol. 124, No. 2, 2002, pp. 242–250.

[32]Su, G., Teng, S., Chen, H. C., and Han, J. C., "Computation of Flow and Heat Transfer in Rotating Rectangular Channels ($AR = 4$) with V-Shaped Ribs by a Reynolds Stress Turbulence Model," American Society of Mechanical Engineers, ASME Paper GT2003–38348, June 2003.